

Application of Tomographic Imaging to Multi-pixel Bolometric Measurements

Y. LIU, N. TAMURA, B.J. PETERSON, N. IWAMA¹⁾, S. KONOSHIMA²⁾,
LHD Experimental Group and the JT-60 team²⁾

National Institute for Fusion Science, Toki 509-5292, Japan

¹⁾*Daido Institute of Technology, Nagoya 457-8530, Japan*

²⁾*Japan Atomic Energy Agency, Naka Fusion Institute, Naka 311-0193, Japan*

(Received 6 December 2006 / Accepted 5 April 2007)

An improved tomographic algorithm in the scheme of Tikhonov-Phillips regularisation method, has been employed for multi-pixel bolometric measurements in order to get as much information as possible while keeping the assumptions to a minimum. The effects of finite detector size have been taken into account with a full three dimensional treatment of the detector geometry. The application of tomographic imaging was implemented to a two-array AXUVD (Absolute eXtreme UltraViolet photodiode) camera on the Large Helical Device (LHD) and a two-dimensional infrared imaging bolometric (IRVB) pinhole camera on JT-60U. Pertinent examples of the results are presented both to illustrate the analysis techniques and to demonstrate the wealth of physics which can be studied.

© 2007 The Japan Society of Plasma Science and Nuclear Fusion Research

Keywords: bolometer, infrared camera, plasma radiation, computed tomography

DOI: 10.1585/pfr.2.S1124

1. Introduction

Various diagnostics for bolometric imaging of plasma have been developed in magnetically confining devices recently including one-dimensional arrays of resistive foil or AXUVD detectors with perpendicular views of plasma in a poloidal cross-section or a two-dimensional multi-pixel IRVB camera with a tangential view of the plasma. While the measurements from such diagnostics are line-integrated along sightlines covering a plasma poloidal cross-section or volume-integrated over solid angle penetrating several poloidal cross-sections, the local emission can be recovered by inverting the data using various assumptions including poloidal or toroidal symmetry and flux surface iso-emissivity. However such assumptions can have an important impact on the results and it is important to make a careful and unbiased assessment of the validity of each assumption. An improved tomographic algorithm in the scheme of Tikhonov-Phillips [1], has been employed for multi-pixel bolometric measurements in order to get as much information as possible while keeping the assumptions to be a minimum in data fitting. The most important features of the improved method are the capability of reconstructing radiation distributions with neither poloidal symmetry nor the flux surface iso-emissivity assumption, built-in smoothing, and useful reconstruction with relatively few detectors. Furthermore, the effects of finite detector size have been taken into account with a full three dimensional treatment of the detector geometry. This

is necessary when the emission of the plasma has a significant variation within the field of view, especially for a tangential viewing camera system. The application of tomographic imaging was implemented to a two-array AXUVD (Absolute eXtreme UltraViolet photodiode) camera on the Large Helical Device (LHD) [2] and a two-dimensional infrared imaging bolometric (IRVB) pinhole camera on JT-60U [3, 4].

2. Hardware

2.1 AXUVD diagnostic

AXUVD is being used on the LHD for measuring the radiation distribution. It allows fast and sensitive measurements of radiated power over a wide range from the near infrared into the soft X ray. Because of the helical coils, the LHD plasma cannot be easily observed from many directions or even from two perpendicular directions in a normal cross-section as it can be done on tokamaks. For the purpose of tomographic imaging of LHD plasma, a system of two 20-channel fan-beam cameras has been arranged in a semi-tangential cross section. These arrays viewed the plasma from the top and the outer port and share the same semi-tangential cross-section to provide a two-dimensional view of the plasma radiation, as shown in Fig. 1, with high temporal (down to 100 μ s) and reasonable spatial (5 cm) resolution of various localized radiative phenomena.

author's e-mail: liu_yi@ms.nifs.ac.jp

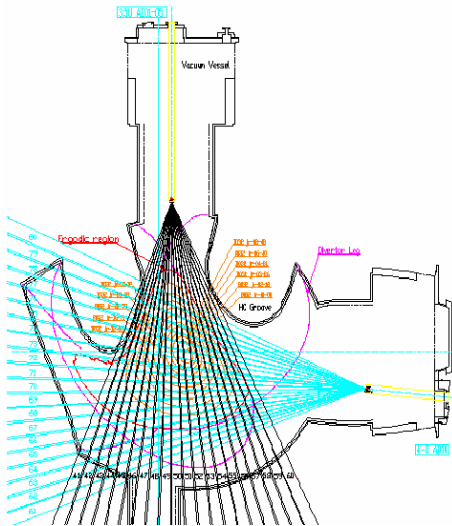


Fig. 1 AXUVD cameras on LHD.

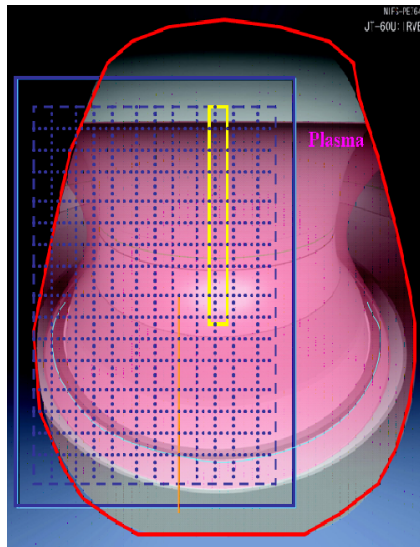


Fig. 2 IRVB FOV in JT-60U.

2.2 Infrared imaging video bolometer

The infrared imaging video bolometer camera system which utilizes a 7 cm × 9 cm × 2.5 micron gold foil and an infrared (IR) camera, was installed at a semi-tangential port on the JT-60U tokamak. The front side of the foil faces the plasma through a 5 × 5 mm square aperture and the backside is viewed by the IR camera to measure the increase in the foil temperature due to the radiation. The IRVB camera provides a 12 (toroidal) × 16 (poloidal) image of the plasma radiation with a sensitivity of 350 μW/cm² and a frame rate of 30 fps. Figure 2 shows the field of view (FOV) of the IRVB installed at a semi-tangential port on the JT-60U tokamak. The semi-tangentially viewing IRVB camera provides a wide-angle plasma coverage with optimized views of the main plasma and the divertor. Since the radiation is integrated along the

line of sight extending toroidally and poloidally, there is always an integration effect and tomographic techniques are then used to unfold the radiation profile.

3. Data Analysis

3.1 Application of linear and nonlinear regularisation on AXUVD measurements

To take full advantage of the available information in limited number of line-integrated AXUVD measurements on LHD, the local radiation emissivity E is obtained by inverting the measured brightnesses with Tikhonov-Phillips regularisation. This regularisation looks for a solution fitting the line-integrated data (M channels) and having minimum curvature, the inversion is obtained upon minimizing the $\gamma R + \|LE - S\|^2/M$, where R is the curvature regularisation term as $R = \int_D [\nabla^2 E(x, y)]^2 dx dy = \|CE\|^2$, L is the response matrix. Parameter γ is set to let $\|\chi\|^2 \approx M$.

Starting from a Tikhonov-Phillips regularization, we add a diagonal weighting matrix F . Here, $F_{jj} = 1/\sqrt{E_j}$ was used, where E_j is the previous solution in iteration. Now, the $\gamma\|CE\|^2$ becomes $\gamma\|F(CE)\|^2$. This is to prevent the oversmoothing of peaks in Tikhonov-Phillips inversion. This technique is based on the minimum Fisher information principle, which assures that regions of low value are particularly smooth, whereas smoothing is less strong where the value is large. It is very suitable for solving the radiation tomography problem, as a localized high emissivity is real in plasma and it is not supposed to smooth this kind of structure. A further advantage of the weighted smoothing is that some artifacts in low value region caused by the nearby high emission can be removed. With the help of tomography methods applied on the high temporal and spatial resolution AXUVD system, a series of tomographic images can be obtained. An example of the image of emission from titanium injected by tracer-encapsulated solid pellet is shown in Figure 3.

3.2 Application of regularisation to IRVB measurements

For the tangential camera on JT-60U, bolometer measurements require a fully three-dimensional treatment of the detector geometry since the effects of finite detector size should be taken into account. A general treatment of arbitrary detector geometry which provides a 3-D field of view analysis with the help of a detector point response calculation [5], is being used to calculate the response matrix. The power incident on a detector from plasma is a volume integral of emissivity and detector response: $I = \iiint \varepsilon(R, Z, \varphi) \frac{S_{\text{det}}}{4\pi D^2} dV$. After discretization, we get the matrix equation in cylindrical coordinates as $I \approx \sum_{i,j,k} \varepsilon_{i,j,k} W_{i,j,k}$, where the detector response matrix element $W_{i,j,k}$ is a volume integral of the detector point response as

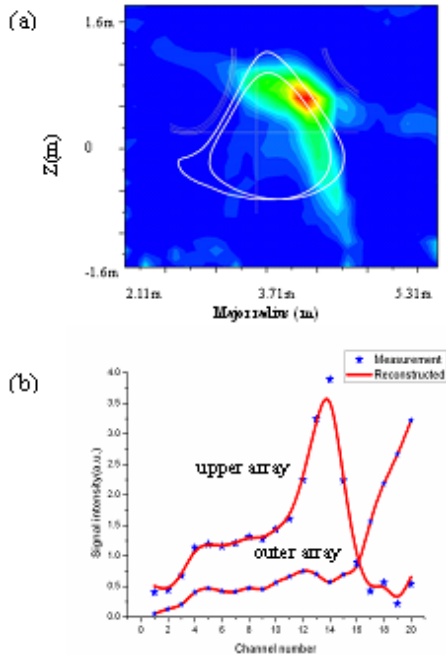


Fig. 3 Highly localized emission profile from titanium tracer injected into the magnetic island region in shot 64880. (a) Reconstructed 2D emission profile with white lines showing the magnetic island structure; (b) Comparison of chord integrated signal from measurement and reconstruction.

$$W_{i,j,k} = \int_{R_i}^{R_i+\Delta R} R dR \int_{Z_j}^{Z_j+\Delta Z} dZ \int_{\varphi_k}^{\varphi_k+\Delta\varphi} g(R, Z, \varphi) d\varphi$$

$$g(R, Z, \varphi) = \iint \frac{dS}{4\pi D^2}.$$

The procedure is to calculate point response first, which involves integration of the distance and angular dependence over the region of overlap between the detector and the projection of the point through the square aperture. Then a 3D integration can be performed in each volume grid ($32 \times 32 \times 360$ in total). It's inefficient and impractical to evaluate detector response for each volume element of the 3-D grid. A search algorithm is used to identify volume elements contained in the detector's FOV.

The tomography algorithm described earlier can be applied to the tangentially viewing IRVB camera on JT-60U tokamak with an assumption of toroidal symmetry. After merging the contribution from pixels in different toroidal positions, a spatially and temporally resolved measurement of the radiation emissivity in a poloidal cross-section can be obtained. It provided reasonable two-dimensional profiles of plasma emission with good agreement with resistive bolometer measurements. The 2D tomography method allows us to investigate in detail the temporal and spatial evolution of the radiated profiles using one tangentially viewing IRVB camera. An example

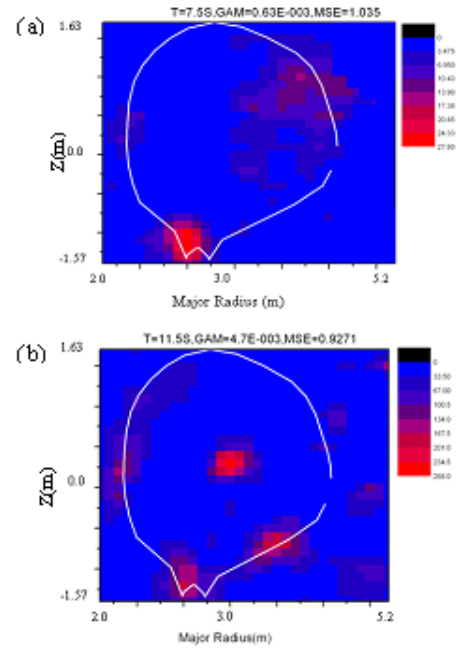


Fig. 4 Emissivity image of poloidal cross-section in JT-60U during shot 45664. Pixel dimension is 10 cm and white line shows the first wall. (a) Emissivity image at $t = 7.5$ s, the radiation comes dominantly from the divertor region. (b) At $t = 11.5$ s, the increase in radiation from the core plasma is due to heavy impurity accumulation.

of the radiation profile reconstruction is shown for standard divertor operation at $t = 7.5$ s in Fig. 4(a). The main feature of the radiation profile is that the radiation comes dominantly from the divertor region, and it is consistent with resistive bolometer measurements. A much different radiation profile results from the increase in radiation from the core plasma at $t = 11.5$ s and is shown in Fig. 4(b). The increase in radiation from the core plasma is due to heavy impurity accumulation. In addition, the divertor radiation has moved down slightly along the inboard divertor from the IRVB measurement, which was also observed by the resistive detectors. Through, some differences between reconstructed and measured chord integrated profiles still existed as seen on the 2D image as bright spots outside the plasma boundary, the tomographic reconstruction can lead one to infer the 2D plasma radiation profile both in the core and divertor from the data of the tangentially viewing IRVB camera.

Acknowledgments

This work has been carried out with financial support from Grant-in-Aid for JSPS Postdoctoral Fellows, Grant-in-Aid for Scientific Research on Priority Areas, No. 16082207, MEXT and budgetary Grant-in-Aid No. NIFS06ULHH524 of the National Institute for Fusion Science, MEXT Grant-in-Aid No. 16560729.

- [1] N. Iwama, "Phenomena in Ionized Gases (XXII ICPIG)", edited by K.H. Becker *et al.*, AIP Press (1996), pp.289-298.
- [2] B.J. Peterson *et al.*, Plasma Phys. Control. Fusion **45**, 1167 (2003).
- [3] S. Konoshima *et al.*, 32nd EPS Conf. on Plasma Phys. and Control. Fusion, ECA Vol. 29C, P-4.092 (2005) (CD-ROM http://eps2005.ciemat.es/papers/pdf/P4_092.pdf)
- [4] B.J. Peterson *et al.*, to be published in J. Nucl. Mater.
- [5] K. Tritz *et al.*, Rev. Sci. Instrum. **77**, 10F510 (2006).